

Experimental determination of the proton escape width in the giant dipole resonance of ^{89}Y

E. Van Camp, R. Van de Vyver, E. Kerkhove, D. Ryckbosch, H. Ferdinande,
P. Van Otten, and P. Berkvens

Laboratorium voor Kernfysica, Rijksuniversiteit Gent, B-9000 Ghent, Belgium

(Received 21 July 1981)

The $^{89}\text{Y}(\gamma, p)^{88}\text{Sr}$ reaction was studied at various bremsstrahlung end point energies in the giant dipole resonance region. Using an artificially constructed pseudomonoeenergetic photon spectrum, it was possible to determine the absolute cross sections for various photoproton reaction channels. From the direct decay cross sections the proton escape width Γ_p^1 of the $T_{<}$ giant dipole resonance was derived; its value amounts to 0.30–0.35 MeV. The nondirect contribution equals about 25% of the total energy-integrated photoproton cross section.

[NUCLEAR REACTIONS $^{89}\text{Y}(\gamma, p)$, $E = 14\text{--}24$ MeV; measured
 $\sigma(E)$ absolutely. Deduced Γ_p^1 . Natural target.]

I. INTRODUCTION

The decay of the electric giant dipole resonance (GDR) was originally assumed to be of a statistical nature. However, it was shown by Lane and Lynn¹ that this statistical mechanism accounts for a cross section in the (γ, p_0) and (γ, n_0) channels which is several orders of magnitude lower than the observed one, at least for medium and heavy nuclei. In order to obtain a better agreement between theory and experiment, these same authors assumed a direct knockout photonuclear process to be important. The fact now that this direct part alone was not sufficient led Brown² and Clement *et al.*³ to the conclusion that a semidirect two-step mechanism should essentially contribute to the (γ, p_0) and (γ, n_0) reactions; in this mechanism the nucleus decays by direct nucleon emission from the intermediate collective dipole state. Subsequently this so-called direct-semidirect (DSD) reaction model was successfully applied for the description of the magnitude of the ground state photonuclear cross sections⁴.

However, the photonuclear disintegration of the nucleus in the GDR region is not due to this DSD mechanism alone. Therefore it is important to gain some knowledge about the decay properties of the GDR as it may lead to a better understanding of the coupling of this simple collective mode to

other degrees of freedom of the excited nucleus. At present, very few experimental data on the decay widths of the GDR are available. It was the aim of the present experiment to determine the cross sections of various fragmentation modes in the $^{89}\text{Y}(\gamma, p)$ channel; this nucleus has a simple structure and the general features of its GDR are well known⁵.

II. PHOTONUCLEAR REACTION MECHANISM

In the region of the electric dipole resonance, the photonuclear reaction process proceeds through two fundamental mechanisms. The most simple one is the direct knockout of a nucleon by a photon; such a process does not yield information about the existence of high-lying collective states in the target nucleus. The cross section for this process then shows a nonresonant behavior since it does not proceed via the excitation of such an intermediate state. In the second mechanism a simple collective 1p-1h doorway state is built up by the absorption of a photon, which is possible due to the one-body nature of the electromagnetic interaction operator. In the case of dipole photon absorption the intermediate state is the well-known Goldhaber-Teller vibration $|D\rangle$ which generates a giant resonance in the photon absorption channel

at $E \simeq 78 A^{-1/3}$ MeV. This resonance has a width of several MeV and consequently the lifetime of the intermediate dipole state is of the order of 10^{-22} s. The damping of this state is due to friction caused by the mutual interaction between nucleons so that particles can be emitted into the continuum. The decay mechanism of this collective doorway state can be divided into three parts corresponding to the number of times the residual interaction has to be applied in the time evolution of the nuclear system before a particle can escape to the continuum. These are the direct, the prestatistical, and the statistical decay mechanisms. Once the collective motion is set up it can directly decay to the continuum, consisting of a free nucleon and a hole state in the residual nucleus, due to the two-body residual interaction acting in the final state channel. The probability for this mechanism gives rise to the escape width Γ^\dagger of the dipole state. On the other hand, the coherent 1p-1h vibrational state can also couple to the more complicated 2p-2h states through this residual force (internal decay). Successive interaction couples these 2p-2h states to more and more complicated np - nh states, leading to the dissipation of the GDR energy over all degrees of freedom. Consequently in the internal decay the initial coherent motion passes into an incoherent motion of many nucleons of which the lifetime is much longer. The thermalization goes on until a nucleon with sufficiently low angular momentum can escape from the nucleus in a statistical way. However, at each stage of this thermalization process nucleons may also escape from the nucleus giving rise to prestatistical decay of the giant resonance. The probability for this internal decay mechanism leads to the spreading width Γ^\ddagger ; it evidently is a function of the density of 2p-2h states in the first stage of the decay. The formation and decay of the GDR is schematically shown in Fig. 1.

The contribution of the various reaction mechan-

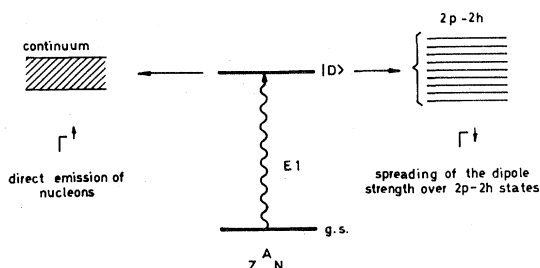


FIG. 1. Schematic representation of the fundamental decay modes of the giant dipole resonance.

isms to the total photoabsorption cross section changes from nucleus to nucleus. However, it is well known that the direct knockout photonuclear process is responsible for only a fraction of the cross section, while the main part originates from the excitation of the dipole vibration. On the other hand, the contribution of each decay mechanism to the total damping width of this dipole state strongly depends on the mass number of the nucleus involved. For medium and heavy nuclei, the damping of the GDR mainly proceeds through spreading of the dipole strength and further dissipation of the energy followed by evaporation of neutrons.⁶⁻⁸ This is due to the fact that the density of 2p-2h and of more complicated states is high in the GDR region of such nuclei while, on the other hand, the high Coulomb and momentum barriers prevent the direct escape of nucleons. For light nuclei the escape width Γ^\dagger is the most important quantity, as was indicated by 1p-1h continuum calculations of the GDR,^{9,10} without absorptive part in the potential. Using this formalism dipole widths equal to about 3, 1, and 0.7 MeV were found for ¹²C, ⁴⁰Ca, and ²⁰⁸Pb, respectively. Notwithstanding the above arguments both spreading and escape contribute to the decay of the giant resonance.

Strictly speaking, the experimental separation of the direct decay from the statistical and prestatistical decay is not possible; however, if the emission of nucleons from the dipole state to the different states in the residual nucleus can be identified, it is feasible to estimate the various partial spreading Γ^\ddagger and escape Γ^\dagger widths. The determination of the cross sections for these photonuclear processes in which the residual nucleus is left in a hole state leads to the partial nucleon escape widths, while the cross sections for the channels where the residual nucleus remains in more complicated states originate from processes with a statistical or prestatistical nature and thus give rise to the spreading width.

As for most nuclei the giant resonance is built up by more than one dipole state, slightly differing in energy, the resonance width is further increased by an amount $\Delta\Gamma$ which does not depend on the spreading or on the nucleon escape of the dipole states involved. Thus the observed width Γ can in general be written as

$$\Gamma = \Gamma^\dagger + \Gamma^\ddagger + \Delta\Gamma .$$

The medium-heavy spherical nucleus ⁸⁹Y, which is reported on in the present paper, has a ground state configuration with a closed $N = 50$ neutron

shell structure and one proton in the $2p_{1/2}$ sub-shell.¹¹ A shell model calculation by Vergados and Kuo¹² shows that the $T_<$ giant resonance of ^{89}Y essentially consists of one dipole state, so that the additional component $\Delta\Gamma$ vanishes. On the other hand, in the $^{89}\text{Y}(\gamma,p)$ reaction, the residual nucleus ^{88}Sr also has a closed $N=50$ shell so that the low-lying excited states in this nucleus consist of proton configurations; most of these are proton-hole states^{11,13,14} and as such, this will make the determination of the direct proton escape from the dipole state possible.

III. EXPERIMENTAL PROCEDURE AND DATA ANALYSIS

For the study of the (γ,p) reaction, a natural ^{89}Y foil with a thickness of 13.3 mg/cm^2 was irradiated with a bremsstrahlung photon beam; photoprotons were detected at seven different angles θ by means of uncooled Si (Li) detectors. The experimental setup was described in detail in a previous paper.¹⁵ Photoproton spectra were measured at several bremsstrahlung end point energies between 14 and 25 MeV, going up in 1 MeV steps. The proton energy calibration procedure and the correction for energy loss were also discussed in a former article,⁵ together with an evaluation of the suitability of the use of the Schiff bremsstrahlung spectrum near the end point energy. An example of a typical photoproton spectrum (without background subtraction), for $\theta=90^\circ$ and at an end point energy of 23 MeV, is shown in Fig. 2; the dashed line represents an extrapolation of the background spectrum.

Since the energy difference between the ground state and the first excited state in the residual nucleus ^{88}Sr equals 1.84 MeV, only the uppermost 1.8 MeV wide interval in each proton spectrum contains pure ground state protons. As on the other hand the second excited state is located about 0.9 MeV above the first one, we were able to extract both the (γ,p_0) and the (γ,p_1) cross sections⁵.

However, in order to use all the information contained in the measured proton spectra, a nearly monoenergetic photon spectrum was constructed artificially by taking an algebraic sum of suitably normalized bremsstrahlung spectra, with consecutive end point energies, in the following way:

$$\phi_M(E_\gamma, T_e) = \phi(E_\gamma, T_e) - a\phi(E_\gamma, T_e - 1 \text{ MeV}) + b\phi(E_\gamma, T_e - 2 \text{ MeV}) .$$

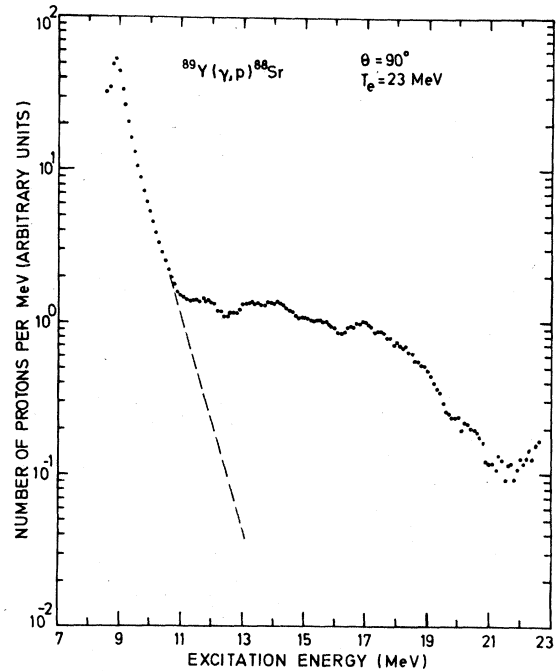


FIG. 2. A 90° photoproton spectrum taken at a bremsstrahlung end point energy of 23 MeV. The horizontal scale represents the excitation energy for ground state proton decay and is defined in the text. The dashed line shows an extrapolation of the exponentially decreasing background.

The function $\phi(E_\gamma, T_e)$ is the Schiff bremsstrahlung spectrum with end point energy T_e ; the parameters a and b are both positive and are chosen in such a way that the function $\phi_M(E_\gamma, T_e)$ represents to a good approximation a monoenergetic spectrum. An example is shown in Fig. 3: its maximum is located at $T_e - 1$ MeV and the FWHM of this photon spectrum nearly equals 0.9 MeV. If one now takes the algebraic sum of the corresponding photoproton spectra, normalized in the same way, a differential proton spectrum is then obtained that corresponds to the above generated monoenergetic photon flux. Consequently, a total integrated-over-angles proton spectrum can be produced by fitting a sum of Legendre polynomials to these differential proton spectra in the usual way:

$$\frac{dN}{dT_p}(E, \theta) = \sum_{i=0}^4 A_i(E) P_i(\cos\theta) .$$

It is clear that the magnitude of such a proton spectrum can easily be converted to an absolute cross section scale. In Fig. 4, two examples of integrated-over-angles photoproton spectra are de-

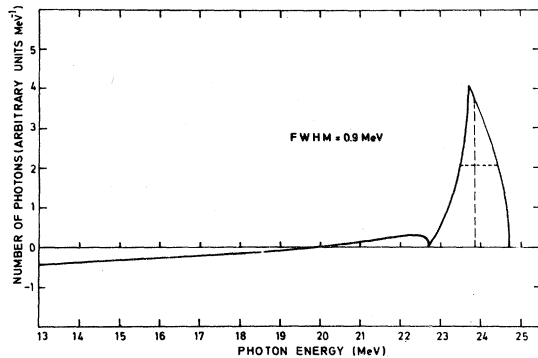


FIG. 3. An example of the pseudomonoenergetic photon spectrum $\phi_M(E_\gamma, T_e)$ for $T_e = 24.7$ MeV, with parameter values $a = 1.37$ and $b = 0.329$.

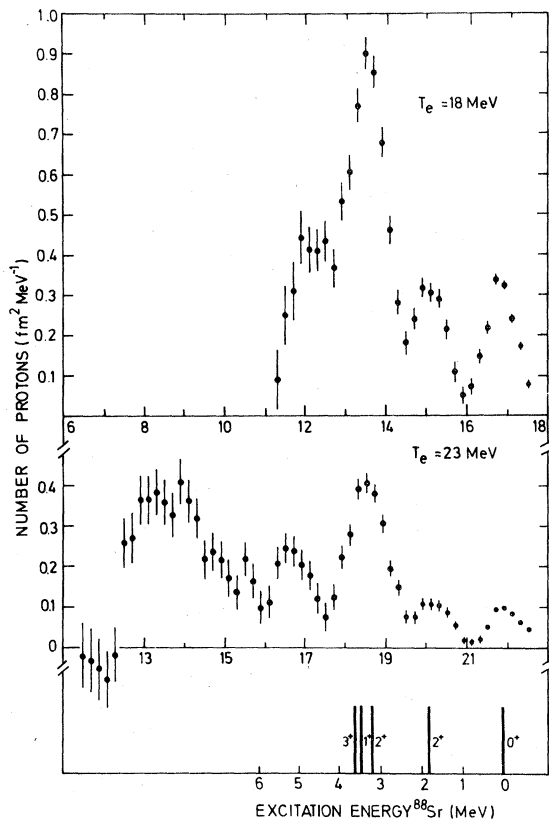


FIG. 4. Normalized ^{89}Y photoproton energy distributions corresponding to a monoenergetic photon spectrum for $T_e = 18$ MeV (upper spectrum) and $T_e = 23$ MeV (lower spectrum); the energy scale for both spectra represents excitation energy for ground state proton decay and is defined in the text. The bottom part of the figure shows the level scheme of the residual nucleus ^{88}Sr where only the proton-hole states are indicated.

pected for T_e equal to 18 and 23 MeV, respectively. The energy T_e at the bottom of each spectrum represents the excitation energy in ^{89}Y as defined by

$$E \simeq \frac{A}{A-1} T_p + S_p,$$

where T_p is the proton kinetic energy and S_p denotes the ground state separation energy ($=7.07$ MeV). However, it should be pointed out here that all protons originate from an excitation energy interval (0.9 MeV wide) centered around 17 and 22 MeV, respectively. The bottom part of the figure shows the excitation energy scale in the residual nucleus ^{88}Sr for which the proton-hole states are indicated. It is important to know to what extent such photoproton spectra, corresponding to a specific excitation energy region, contain all protons that are emitted by the ^{89}Y nucleus. Now, since the penetrability of 4 MeV protons is at most 6%, as calculated by Mani *et al.*¹⁶ using an optical model potential, almost no protons with a lower energy can escape from ^{89}Y . As is indicated by Fig. 2, the background contribution to the original proton spectra, which has a nearly exponentially decreasing and structureless behavior, dominates at the low energy end. From $T_p \simeq 4$ MeV upwards this background becomes less important so that one can expect to observe real protons from an excitation energy (as defined by the above expression) equal to 11 MeV onwards; as a consequence this means that the artificial proton spectra (Fig. 4) should only show photoprotons from this excitation energy on and, as this is the case, it indicates that to a good approximation these spectra contain the total number of protons originating from the pseudomonoenergetic photon peak.

IV. RESULTS AND DISCUSSION

As has been mentioned before, the nature of the residual nuclear state determines to a large extent the decay mechanism by which this state can be reached. Below 4 MeV, the excited levels in ^{88}Sr are expected mainly to consist of proton configurations since the energy separation between the closed $N = 50$ neutron shell and the next unfilled $2d_{5/2}$ single particle level has about this value. The excited states of ^{88}Sr have been well studied, both experimentally¹⁷ and theoretically.¹³ By means of the $^{89}\text{Y}(d, ^3\text{He})^{88}\text{Sr}$ pickup reaction only five proton-hole states have been identified, all located below 4 MeV. These are listed in Table I,

together with their single particle configurations.

The low-lying levels in ^{88}Sr are depicted in Fig. 5 in which the proton-hole states are shown separately. The lowest two 2^+ states, located at 1.836 and 3.218 MeV consist of the indicated configurations for 80% and 60%, respectively (Table I). The first one also has a collective behavior as indicated by the enhanced transition strengths measured in (α, α') , (p, p') , and (e, e') experiments.¹⁷ The 3^- level at 2.734 MeV has a collective character and is not excited in the $(d, ^3\text{He})$ reaction. The positive parity states below 4 MeV, not excited by proton pickup, may have a complicated proton configuration relative to the 1p-1h character of the ^{89}Y GDR. Above 4 MeV a large number of states are excited by the $^{87}\text{Sr}(d, p)^{88}\text{Sr}$ and $^{86}\text{Sr}(t, p)^{88}\text{Sr}$ neutron stripping reactions,^{18,19} which means that these states have 1p-1h and 2p-2h neutron configurations; they are complicated states with respect to the proton decay of the dipole state of ^{89}Y .

As explained earlier, direct decay of the GDR leads to hole states in the residual nucleus. However, in the ground state channel, about 10% of the observed cross section is expected to originate from a direct knockout process^{2,3} while, on the other hand, at the lower energy edge of the GDR in this channel a statistical contribution may be important^{4,20} due to the fact that, in this energy region, very few decay channels are open. Although we can expect these same mechanisms to contribute to the cross section for all residual states with a large hole component, it is assumed that the statistical and the direct knockout processes are negligible in the proton-hole channels. Regardless of the fact that this causes the result to be incorrect by about 10%, this assumption enables us to determine the proton escape width Γ_p^1 of the ^{89}Y GDR.

As is evident from Fig. 4, proton channels can be separated which correspond to the 0^+ ground

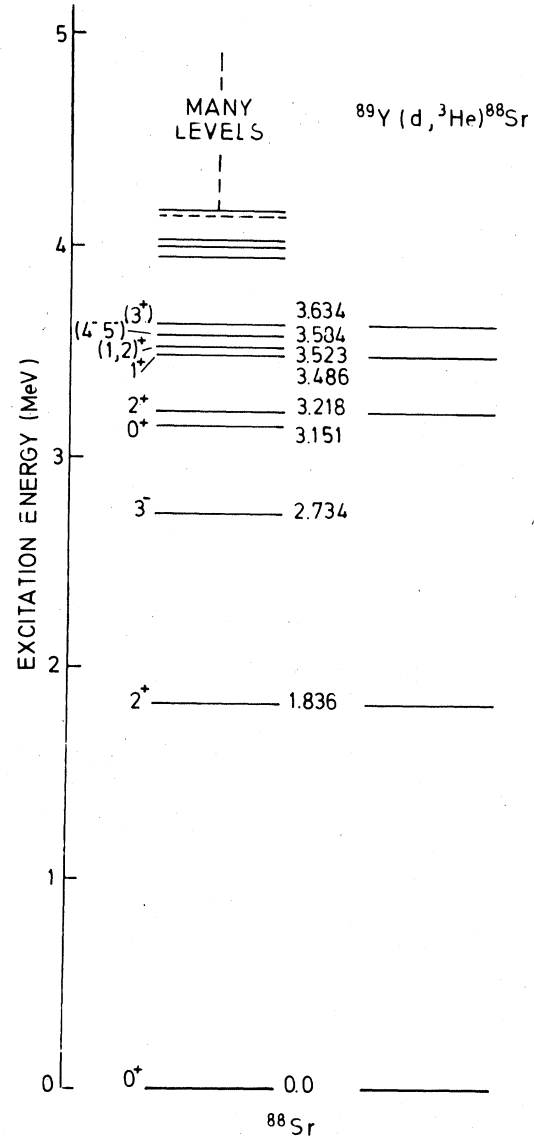


FIG. 5. Level scheme of the low-lying levels in ^{88}Sr ; the proton-hole states identified in the $^{89}\text{Y}(d, ^3\text{He})^{88}\text{Sr}$ reaction are indicated on the right.

TABLE I. Configuration of the proton-hole states in ^{88}Sr ; for the notation reference is made to the closed 0^+ shell model configuration of ^{90}Zr .

| Energy (MeV) | Spin J^π | Configuration |
|--------------|--------------|---|
| 0.0 | 0^+ | $\sqrt{0.7}(2p_{1/2})^{-2} + \sqrt{0.2}(2p_{3/2})^{-2} + \sqrt{0.1}(1f_{5/2})^{-2}$ |
| 1.836 | 2^+ | $a[(2p_{3/2})^{-1}(2p_{1/2})^{-1}]_{2^+} + b[(1f_{5/2})^{-1}(2p_{1/2})^{-1}]_{2^+}$ |
| 3.218 | 2^+ | $c[(2p_{3/2})^{-1}(2p_{1/2})^{-1}]_{2^+} + d[(1f_{5/2})^{-1}(2p_{1/2})^{-1}]_{2^+}$ |
| 3.486 | 1^+ | $[(2p_{3/2})^{-1}(2p_{1/2})^{-1}]_{1^+}$ |
| 3.634 | 3^+ | $[(1f_{5/2})^{-1}(2p_{1/2})^{-1}]_{3^+}$ |

state of ^{88}Sr , to the first excited 2^+ state located at 1.836 MeV and to the group consisting of the three proton-hole states with energies of 3.218 (2^+), 3.523 (1^+), and 3.634 (3^+) MeV. These latter three levels cannot be separated in our experimental results due to the limited energy resolution, which is mainly determined by the FWHM of the artificially constructed monoenergetic photon spectrum. Nevertheless, due to the proton-hole nature of the residual states, these protons must also originate from a semidirect photonuclear process. From the same figure it is also clear that nearly no protons are observed leaving ^{88}Sr in the second excited (3^-) state located at 2.734 MeV. The same is assumed to be true for the channels corresponding to the other non-proton-hole states below 4 MeV excitation energy. In the lower spectrum of Fig. 4 (corresponding to a higher excitation energy in ^{89}Y) a lot of photoprotons is observed for channels in which ^{88}Sr is left in excited states higher than 4 MeV; from this energy onwards the density of states in the residual nucleus is rather high. The photoprotons observed here are emitted in a non-direct decay process of the GDR. From the measured proton spectra cross sections can be derived for each fragmentation mode that can be separated. In the excitation energy interval from 14 to 24 MeV, the cross sections for the reactions wherein ^{88}Sr is left in the ground state, in the first excited state and in the group consisting of the other three proton-hole states near 3.4 MeV are shown in Fig. 6, together with the cross section for the processes in which ^{88}Sr remains in excited states higher than 4.5 MeV. The fact that the various cross sections start from slightly different energy values is due to the different separation energies and the Coulomb barrier.

The absolute magnitude of the cross sections for the (γ, p_0) and (γ, p_1) channels agrees very well with the directly determined one.⁵ The maxima of the cross sections for the three direct-decay channels are located around 16.8 MeV; this is the ^{89}Y giant dipole resonance energy as measured in the (γ, n) experiments of Leprêtre *et al.*,²¹ and Berman *et al.*,²² and in the photon scattering work of Arenhövel and Maison.²³ On the other hand, the maximum in the $[\gamma, p(E > 4.5 \text{ MeV})]$ cross section is situated near 21.5 MeV which corresponds to the energy of the coherent $T_>$ dipole state, expected around 21.2 MeV according to the relation of Akyüz and Fallieros²⁴ for isospin splitting. The integrated cross sections for the different (γ, p) fragmentation modes are summarized in Table II

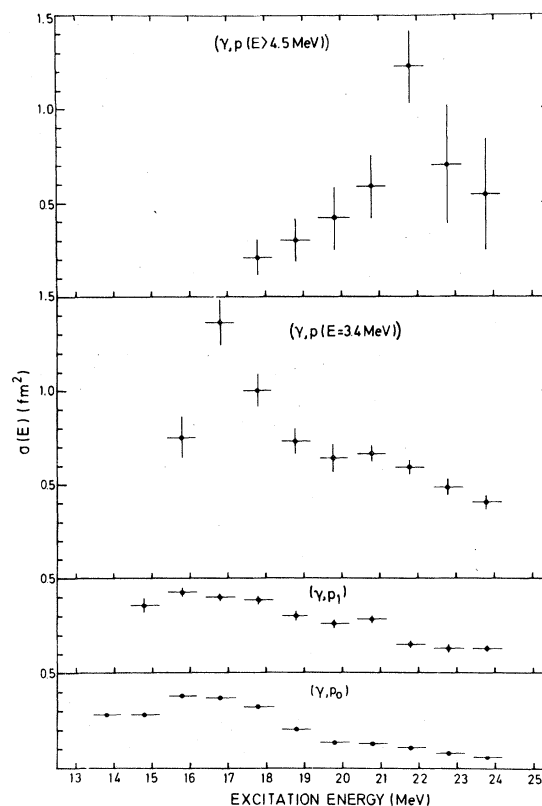


FIG. 6. The absolute $^{89}\text{Y}(\gamma, p)$ cross sections for the various proton channels which could be identified.

together with their relative contribution to the integrated total photoproton cross section, which was obtained by summing the individual cross sections.

Although the giant resonance of ^{89}Y mainly decays following a statistical process (by the evaporation of neutrons), only about 25% (see Table II) of the (γ, p) cross section between 14 and 24 MeV is due to this mechanism. This can be explained by the fact that statistical proton decay is strongly hindered by the Coulomb barrier. From Fig. 6 it is observed that the $T_<$ giant resonance nearly exclusively decays in a direct way in the proton channel, while the nondirect decay is mainly located at an energy where the $T_>$ resonance is expected.

In Fig. 7 the ratio of this nondirect part to the total (γ, p) cross section is illustrated. Above 21 MeV about 50% of the proton decay is due to statistical and prestatistical mechanisms. The large contribution of the nondirect cross section around 21.5 MeV can be understood in terms of the presence of the $T_>$ collective state at this energy; the approximate validity of isospin conservation

TABLE II. Integrated cross sections for the various photoproton channels observed in the $^{89}\text{Y}(\gamma, p)$ reactions.

| Channel | Integration limits | $\int_{E_1}^{E_2} \sigma(E) dE$ (MeV fm ²) | $\frac{\int \sigma(p_i, E) dE}{\int \sigma(p, E) dE} \times 100$ |
|-------------------------------------|---------------------------|---|--|
| | E_1 (MeV) – E_2 (MeV) | | |
| (γ, p_0) | 13.8 – 24.6 | 2.45 ± 0.02 | 15.6 |
| (γ, p_1) | 15.1 – 24.4 | 2.77 ± 0.03 | 17.7 |
| $[\gamma, p (E = 3.4 \text{ MeV})]$ | 15.8 – 23.8 | 6.59 ± 0.18 | 42.1 |
| $[\gamma, p (E > 4.5 \text{ MeV})]$ | 17.8 – 23.8 | 3.86 ± 0.57 | 24.6 |
| $(\gamma, p)_{\text{total}}$ | 13.8 – 24.6 | 15.67 ± 0.60 | 100.0 |

hinders the statistical decay of this state by neutron emission, so that statistical proton emission will be favored. Finally, let us point out that the cross sections for the three proton-hole channels show a bump centered around 21.5 MeV which is also an indication of the existence of the $T_>$ dipole resonance in ^{89}Y .

As mentioned before, the total width Γ of the $T_<$ GDR of ^{89}Y , which is nearly equal to 4 MeV,^{21,22} consists of the spreading width Γ^{\dagger} and the escape width Γ^{\ddagger} . If one now assumes that the total photoabsorption cross section approximates the sum of the (γ, n) and (γ, p) cross sections, then the proton escape width Γ_p^{\ddagger} of the $T_<$ GDR can be derived using the relation

$$\Gamma_p^{\ddagger} = \frac{\sigma_{<}^{\text{SD}}(\gamma, p)}{\sigma_{<}(\gamma, n) + \sigma_{<}(\gamma, p)} \Gamma,$$

where the symbol σ represents the maximum of the Lorentz line fitted to the specific $T_<$ cross section. It should be noted here that the semidirect (SD) photoproton cross section $\sigma_{<}^{\text{SD}}$ equals the sum of the cross sections for the decay processes of the

$T_<$ GDR leading to the proton-hole states and, since the nondirect $\sigma_{<}^{\text{ND}} \simeq 0$ (Fig. 7), we obtain $\sigma_{<}(\gamma, p) \simeq \sigma_{<}^{\text{SD}}(\gamma, p)$, the former having a value of about 1.8 fm². Consequently the proton escape width Γ_p^{\ddagger} amounts to 0.30 or 0.35 MeV, its value depending on whether the (γ, n) cross section of Leprêtre *et al.*²¹ or of Berman *et al.*,²² respectively, has been used.

On the other hand, a value for the nonstatistical neutron decay width of ^{89}Y , containing the neutron escape width Γ_n^{\ddagger} together with a fraction of the spreading width Γ^{\dagger} due to the presence of the prestatistical decay, has recently been published.²⁵ Its magnitude amounts to about 0.8 MeV which represents an upper limit for the neutron escape width Γ_n^{\ddagger} . Taking into account our Γ_p^{\ddagger} result, the experimental total nucleon escape width is restricted to $\Gamma^{\ddagger} \leq 1.1$ MeV. As a consequence, a lower limit for the spreading width is obtained resulting in $\Gamma^{\dagger} \geq 2.9$ MeV. This latter value can be compared with the theoretical estimate⁷ of 3 MeV that was found for ^{90}Zr , a nucleus which has nearly the same GDR characteristics^{21,22} as ^{89}Y and for which the dipole strength is also almost entirely concentrated in one state²⁶.

V. CONCLUSIONS

It can be concluded from our $^{89}\text{Y}(\gamma, p)$ experiments that, with the use of the artificially constructed pseudomonoeenergetic photon spectrum, we were able to determine with reasonable accuracy the cross sections for the decay to the three proton-hole channels together with the cross section for the processes wherein the residual nucleus is left in excited states above 4.5 MeV. These results show that the $T_<$ giant dipole resonance in

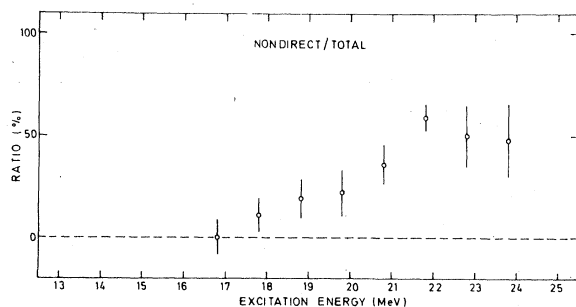


FIG. 7. The ratio of the nondirect to the total cross section for the $^{89}\text{Y}(\gamma, p)$ reaction, as a function of excitation energy.

^{89}Y mainly decays by a direct mechanism (i.e., a semidirect photonuclear reaction process) in the proton channel while the $T_{>}$ dipole state has a large nondirect proton-decay contribution. The $T_{<}$ proton escape width Γ_p^\dagger has a value of 0.30 – 0.35 MeV, whereas the estimated total nucleon escape width Γ^\dagger has an upper limit equal to 1.1 MeV; as such it represents at most 28% of the total damping width of the ^{89}Y dipole state, confirming the dominance of the spreading width in this mass region.

ACKNOWLEDGMENTS

We wish to thank Professor A. J. Deruytter for his continuing interest during the course of this work. We are especially grateful to Dr. R. Carchon and Dr. J. Devos for their valuable help during the initial stage of this work. We also acknowledge the financial support lent by the Interuniversity Institute for Nuclear Sciences (I.I.K.W.) and the National Fund for Scientific Research (NFWO), Brussels, Belgium.

-
- ¹A. N. Lane and J. E. Lynn, *Nucl. Phys.* **11**, 646 (1959).
²G. E. Brown, *Nucl. Phys.* **57**, 339 (1964).
³C. F. Clement, A. M. Lane, and J. R. Rook, *Nucl. Phys.* **66**, 273 (1965).
⁴A. Lindholm, L. Nilsson, M. Ahmad, M. Anwar, I. Bergqvist, and S. Joly, *Nucl. Phys.* **A339**, 205 (1980).
⁵E. Van Camp, R. Van de Vyver, H. Ferdinande, E. Kerkhove, R. Carchon, and J. Devos, *Phys. Rev. C* **22**, 2396 (1980).
⁶M. Danos and W. Greiner, *Phys. Rev.* **138B**, 876 (1965).
⁷E. D. Mshelia, K. Roos, and W. Greiner, *Nucl. Phys.* **A212**, 157 (1973).
⁸A. M. Davidson, *Nucl. Phys.* **A180**, 208 (1972).
⁹M. Marangoni and A. M. Saruis, *Nucl. Phys.* **A132**, 649 (1969).
¹⁰R. F. Barrett and P. P. Delsanto, *Nucl. Phys.* **A173**, 641 (1971).
¹¹C. D. Kavaloski, J. S. Lilley, D. C. Shreve, and N. Stein, *Phys. Rev.* **161**, 1107 (1967).
¹²J. D. Vergados and T. T. S. Kuo, *Nucl. Phys.* **A168**, 225 (1971).
¹³T. A. Hughes, *Phys. Rev.* **181**, 1586 (1969).
¹⁴J. F. Harrison and J. C. Hiebert, *Nucl. Phys.* **A185**, 385 (1972).
¹⁵R. Carchon, R. E. Van de Vyver, H. Ferdinande, J. Devos, and E. Van Camp, *Phys. Rev. C* **14**, 456 (1976).
¹⁶G. S. Mani, M. A. Melkanoff, and I. Iori, Commissariat à l'Énergie Atomique Report, CEA-R-2379, 1963.
¹⁷R. L. Bunting and J. J. Kraushaar, *Nucl. Data Sheets* **18**, 87 (1976).
¹⁸E. R. Cosman and D. C. Slater, *Phys. Rev.* **172**, 1126 (1968).
¹⁹R. C. Ragaini, J. D. Knight, and W. T. Leland, *Phys. Rev. C* **2**, 1020 (1970).
²⁰I. Bergqvist, B. Pålsson, L. Nilsson, A. Lindholm, D. M. Drake, E. Arthur, D. K. McDaniels, and P. Varghese, *Nucl. Phys.* **A295**, 256 (1978).
²¹A. Leprêtre, H. Beil, R. Bergère, P. Carlos, A. Veyssièrè, and M. Sugawara, *Nucl. Phys.* **A175**, 609 (1971).
²²B. L. Berman, J. T. Caldwell, R. R. Harvey, M. A. Kelly, R. L. Bramblett, and S. C. Fultz, *Phys. Rev.* **162**, 1098 (1967).
²³H. Arenhövel and J. M. Maison, *Nucl. Phys.* **A147**, 305 (1970).
²⁴R. O. Akyüz and S. Fallieros, *Phys. Rev. Lett.* **27**, 1016 (1971).
²⁵S. Cardman, *Nucl. Phys.* **A354**, 173c (1981).
²⁶D. Drechsel, J. B. Seaborn, and W. Greiner, *Nucl. Phys.* **A94**, 698 (1967).